The scanning and voxellisation of complex 3D objects for incorporation within Finite Difference Time Domain based acoustic prediction

Ian Drumm

The University of Salford, C.S.E., Salford University, The Crescent, M5 4WT Manchester, UK
i.drumm@salford.ac.uk

This paper presents techniques developed to incorporate complex 3D objects within the author's own Finite Difference Time Domain based acoustic prediction application. Using a combination of 3D laser scanning, ray based voxellisation and a least pth norm based filter design approach to emulate the absorption profiles of non rigid boundaries; complex objects can be incorporated into a variety of acoustic prediction scenarios. The paper will evaluate the success of the approach and explore its application.

1 Introduction

This paper will discuss the laser scanning and voxelisation of arbitrarily shaped objects for use within the author's 3D Finite Difference Time Domain (FDTD) based acoustic prediction software ('Wave Tank'). The author will also demonstrate his approach to modelling arbitrary frequency dependant absorption profiles assigned to the surfaces elements of the voxellised objects.

Originally developed as a computational electrodynamics modelling technique [1], FDTD has found popularity in modelling broadband sound propagation phenomena [2] including frequency dependant absorption, diffraction and interference. The acoustic implementation of FDTD considers sound propagation as coupled equations Eq.(1) and Eq.(2).

$$\frac{\partial u}{\partial t} = -\frac{1}{\rho}\nabla p \qquad (1)$$

$$\frac{\partial p}{\partial t} = -K\nabla \cdot w \qquad (2)$$

where p is pressure, w is particle velocity, ρ is the density of medium and K the bulk modulus. Writing equations Eq.(1) and Eq.(2) in centre difference forms gives equations Eq.(3) Eq.(4) Eq.(5) and Eq.(6) where *i*, *j* and *k* represent grid locations and *n* represents time steps.

$$w_x^{n+1}\left(i+\tfrac{1}{2},j,k\right) = w_x^{n}\left(i+\tfrac{1}{2},j,k\right) - \frac{\delta t}{\rho\delta x}\left\{p^{n+\frac{1}{2}}(i+1,j,k) - p^{n+\frac{1}{2}}(i,j,k)\right\}$$
(3)

$$w_y^{n+1}\left(i,j+\tfrac{1}{2},k\right) = w_y^{n}\left(i,j+\tfrac{1}{2},k\right) - \frac{\delta t}{\rho\delta y}\left\{p^{n+\frac{1}{2}}(i,j+1,k) - p^{n+\frac{1}{2}}(i,j,k)\right\}$$
(4)

$$w_z^{n+1}\left(i,j,k+\tfrac{1}{2}\right) = w_z^{n}\left(i,j,k+\tfrac{1}{2}\right) - \frac{\delta t}{\rho\delta z}\left\{p^{n+\frac{1}{2}}(i,j,k+1) - p^{n+\frac{1}{2}}(i,j,k)\right\}$$
(5)

$$p^{n+\frac{1}{2}}(i,j,k) = p^{n-\frac{1}{2}}(i,j,k) - K\delta t\left\{\frac{w_x^n\left(i+\tfrac{1}{2},j,k\right) - w_x^n\left(i-\tfrac{1}{2},j,k\right)}{\delta x} + \frac{w_y^n\left(i,j+\tfrac{1}{2},k\right) - w_y^n\left(i,j-\tfrac{1}{2},k\right)}{\delta y} + \frac{w_z^n\left(i,j,k+\tfrac{1}{2}\right) - w_z^n\left(i,j,k-\tfrac{1}{2}\right)}{\delta z}\right\}$$
(6)

Hence the medium is effectively represented as interleaved 3D grids of pressure and velocities respectively with neighbouring pressure and velocity nodes separated by a half step. To avoid reflections at grid terminations Perfectly Matched Layers (PMLs) [3] are implemented to introduce gradual absorption whilst keeping the impedance constant. By adding or setting pressures within specified grid positions various source types can be emulated. Though to implement sources that are 'transparent' (i.e. don't scatter incident waves yet preserve the desired driving function) the impulse response of the medium must effectively be removed from the source driving function [4].

2 Voxelisation

Voxellisation parses complex 3D data to extract plane and absorption data (if provided) which is hence used to set corresponding elements within the 3D FDTD grid. Data types parsed by the author's software include X3D, ODEON and CATT. Note X3D is a popular export format from common 3D file creation software and thus allows the author to utilise a wider range of formats including DFX, 3D Studio Max, Google Sketch up, etc. Although there are some fast voxelisation techniques documented in computer graphics literature the author uses a simple ray based approach describe here. Consider a plane given by its vertices $\mathbf{p}_i$ where i indexes into an array of N vertices such that $i = 0,1,2,3...N-1$. The plane can also be described by the equation

$$D = \hat{\mathbf{n}} \cdot \mathbf{p} \qquad (7)$$

where p is a point the plane and D is a constant scalar and $\hat{\mathbf{n}}$ is the plane's unit normal found using the vector cross product

$$\mathbf{n} = (\mathbf{p}_2 - \mathbf{p}_1)\times(\mathbf{p}_0 - \mathbf{p}_1). \qquad (8)$$

Also consider a ray $\mathbf{r}$ such that

$$\mathbf{r} = \mathbf{s} + \mathbf{c}t \tag{9}$$

where s is the start vector position, c is the direction vector, and t a scalar distance or time value. The ray intersects the plane at

$$t = \frac{D - \hat{\mathbf{n}} \cdot \mathbf{s}}{\hat{\mathbf{n}} \cdot \mathbf{c}} \tag{10}$$

This gives the point of intersection $\mathbf{r}$ which can be tested as to whether it's within the plane's boundary by considering the normal vectors $\mathbf{n}_i$ formed with respect to $\mathbf{r}$ and all adjacent plane vertices $\mathbf{p}_i$ and $\mathbf{p}_{i+1}$ such that

$$\mathbf{n}_i = (\mathbf{p}_i - \mathbf{r}) \times (\mathbf{p}_{i+1} - \mathbf{r}) \tag{11}$$

If the sense of all dot products

$$dp = \hat{\mathbf{n}} \cdot \hat{\mathbf{n}}_i \tag{12}$$

are consistent then the point is within the plane boundary.

For each empty FDTD grid element found to correspond to a ray/plane intersection; parameters are set to indicate appropriate reflecting properties. Fig.1 shows an example of such a ray fired at a plane.

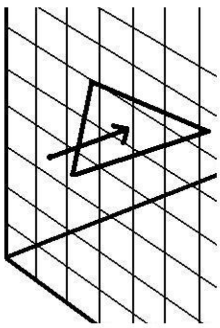

Fig.1. A ray is fired at plane to test if it corresponds with a voxel of the grid

3 Emulating frequency dependant absorption

The author's approach to emulating frequency dependant absorption utilises octave banded absorption coefficients to specify the magnitude response of filters. These filter's IIR coefficients are hence computed via a quasi-netwon based optimisation technique. An assumption was made that a velocity component at a surface element can be given as a function of the history of normal velocity components incident and the history previous outputs from this function, for example…

$$w = f_n\left(n_x \cdot w_x^n, n_x \cdot w_x^{n-1}, n_x \cdot w_x^{n-2} ..., f_{n-1}(...), f_{n-2}(...),..\right)$$
(13)

where w_x^n is given by Eq.(3) and n_x is the x component of the surface's absolute unit normal. The output w velocity becomes an input argument to equation 6 hence the approach suggested is easy to integrate into the FDTD iterative cycle. The Eq.(13) is in effect the difference equation of an IIR filter which could written as

$$w = \left[h_0 + \sum_{i=1}^{N} b_i w_{n-i} - \sum_{j=1}^{N} a_j f_{n-j} \right] \tag{14}$$

The filter coefficients $h_0, a_1, a_2, ...a_N \quad b_0, b_1, b_2, ...b_N$ can be found from the plane's octave banded absorption coefficients $\alpha(\omega)$ where

$$\omega = {}^{125}\!/_{2\pi}, {}^{250}\!/_{2\pi}, ..., {}^{4000}\!/_{2\pi}$$

The author's implementation considers transmission coefficients such that Eq.(15) is the desired magnitude response of a filter.

$$H_d(\omega) = 1 - \sqrt{1 - \alpha(\omega)} \tag{15}$$

A least pth norm based filter design approach was hence employed to find the desired coefficients. The approach employ's Newton method in optimisation to find $\mathbf{x} = [h_0, a_1, a_2 ... a_N, b_1, b_2 ... b_N]^T$ from the minimised the Lp-norm objective function

$$E(\mathbf{x}) = \int \left| H(\omega) - H_d(\omega) \right|^2 d\omega \tag{16}$$

where

$$H(\omega) = h_0 \frac{B}{A} \tag{17}$$

$$B = 1 + b_1 z^{-1} + b_2 z^{-2} + ... + b_N z^{-n}$$

$$A = 1 + a_1 z^{-1} + b_2 z^{-2} + ... + a_N z^{-n}$$

It can be shown [5] that the gradient of the error function in Eq.(16) is

$$\nabla E(\mathbf{x}) = 2\int \mathrm{Re}\left[\left(H(\omega) - H_d(\omega)\right)^* \nabla H(\omega)\right] d\omega \quad (18)$$

and

$$\nabla H(\omega) = \left[\frac{\partial H}{\partial x_1}, \ldots, \frac{\partial H}{\partial x_m}\right] \quad (19)$$

where the corresponding derivatives with respect to elements of $\mathbf{x}$ are given by

$$\frac{\partial H}{\partial x_m} = \frac{H(\omega)}{h_0}\{m = 1 \quad (20)$$

$$\frac{\partial H}{\partial x_m} = -\frac{H(\omega)z^{-m-1}}{1+A}\{1 < m < N+1 \quad (21)$$

$$\frac{\partial H}{\partial x_m} = \frac{H(\omega)z^{-m-1-N}}{1+B}\{N+1 < m < 2N+1 \quad (22)$$

Similarly the Hessian matrix can be given by Eq.(23) with component derivatives of the matrix easily evaluated.

$$\nabla^2 E(\mathbf{x}) = 2\int 2\,\mathrm{Re}\left[\left(H(\omega) - H_d(\omega)\right)^* \nabla^2 H(\omega) + \nabla H^* \nabla H^T\right] d\omega$$

(23)

An iterative scheme (Eq.(24)) can be applied to minimise the error function and hence give filter coefficients approximating towards the desired response where $0 < \alpha < 1$, $\beta \approx 3$, $k = 0,1,2,3\ldots iterations$.

$$\mathbf{x_{k+1}} = \mathbf{x_k} + \alpha\left(\nabla^2 E + \beta I\right)^{-1} \nabla E \quad (24)$$

However for reasons of computational efficiency the author later adopted a Quasi-Newton approach that uses an approximation of the inverse Hessian matrix $\mathbf{B_k}$. Here the iterative scheme can be written as

$$\mathbf{x_{k+1}} = \mathbf{x_k} - \alpha_k \boldsymbol{\delta}_\mathbf{k} \quad (25)$$

where the descent direction

$$\boldsymbol{\delta}_\mathbf{k} = -\mathbf{B_k} \nabla \mathbf{E_k} \quad (26)$$

The step size α_k is found by a line search to ensure the descent satisfies Wolfe conditions and hence gives sufficient decrease. By considering a change in gradient

$$\boldsymbol{\gamma}_\mathbf{k} = \nabla \mathbf{E_{k+1}} - \nabla \mathbf{E_k} \quad (27)$$

the Davidon-Flecture-Powell update formula (Eq.(28)) was employed changing $\mathbf{B}$ every iteration from an initial identity matrix assumption.

$$\mathbf{B_{k+1}} = \mathbf{B_k} + \frac{\boldsymbol{\delta}_\mathbf{k} \boldsymbol{\delta}_\mathbf{k}^\mathbf{T}}{\boldsymbol{\gamma}_\mathbf{k}^\mathbf{T} \boldsymbol{\delta}_\mathbf{k}} - \frac{\mathbf{B_k} \boldsymbol{\gamma}_\mathbf{k} \boldsymbol{\gamma}_\mathbf{k}^\mathbf{T} \mathbf{B_k}}{\boldsymbol{\gamma}_\mathbf{k}^\mathbf{T} \mathbf{B_k} \boldsymbol{\gamma}_\mathbf{k}} \quad (28)$$

An outline of the Quasi Newton approach is given in [6] though readers interested implementing in C++, C#, Java, etc may instead choose efficient third party generic optimisation classes, e.g. [7] in conjunction with Eq.(16) to Eq.(22).

4 3D Laser Scanning

As well as utilising a 3D data from the huge range of repositories available the author has explored 3D laser scanning as a way implementing more specific prediction scenarios. A Konica Minolta VI-910 3D laser scanner was used. The equipment allowed one to place a figurine on a rotating plate and hence take a series of eight or so scans at varying side angles. A top down scan was also needed. Using Doppler laser interferometry the device is able to generate list of appropriately positioned polygons. Similar points indentified on the scans (e.g. tips of ears, toes and eyes) were subsequently manually registered to allow the scanner's software to knit together the separate scans and fill any remaining gaps to create a full 3D representation of the mouse. The 3D file was hence saved and converted to X3D, a file format that can be parsed by the author's 'Wave Tank' application. Note the mouse consisted of some 79000 triangles.

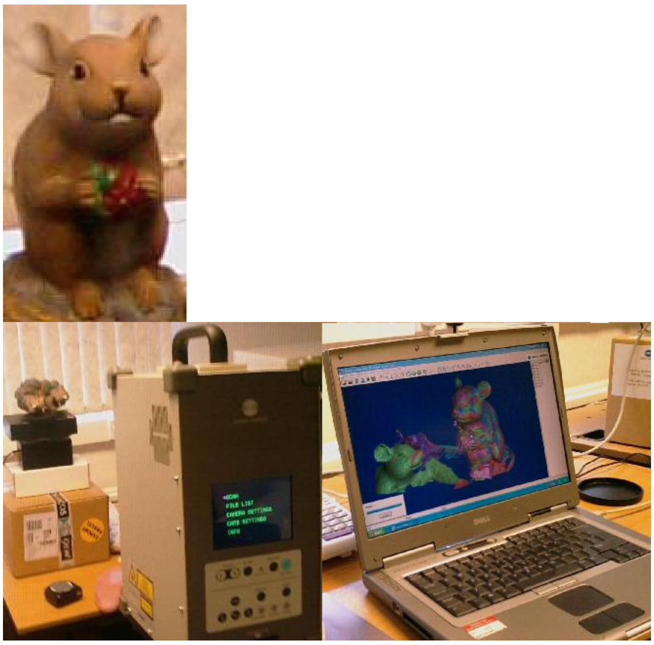

Fig.2. Mouse figurine being scanned and 3D Laser scanner

5 FDTD emulated sound propagation

Fig.3. has plan, elevations and a 3D view of the FDTD predicted sound field approaching the mouse.

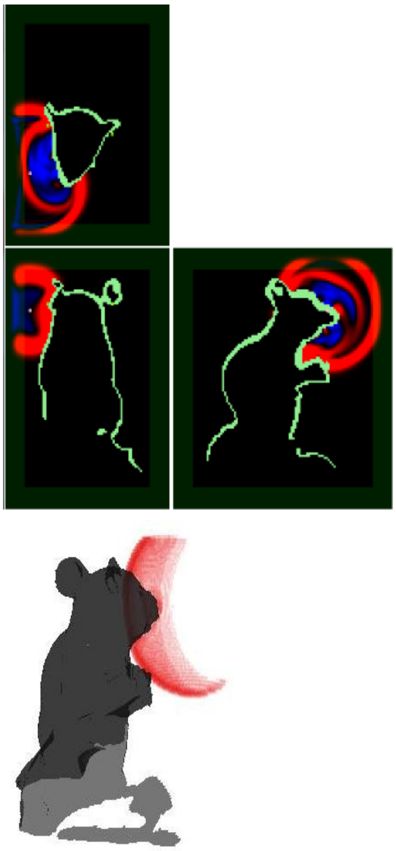

Fig.3. A 3D view and side views of simulation.

By placing a Gaussian pulse source at varying points in front of the mouse and detectors near the mouse's ears; one can demonstrate the technique's potential for say predicting the binaural hearing of the mouse. Fig.4 shows the record pressure responses at the mouse's separate ears.

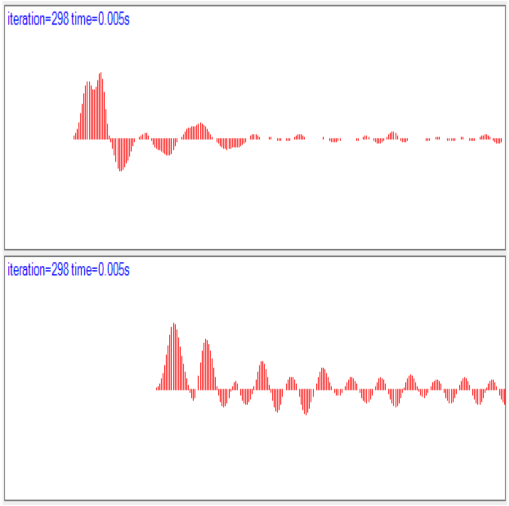

Fig.4. Pressure impulse responses at ears of mouse in 'Wave Tank' prediction.

References

[1] K. S. Yee, "Numerical solution of initial boundary value problems involving Maxwell's equations

in isotropic media," IEEE Trans. Antennas Propagat. 14, 302–307 (1966).

[2] J.G. Meloney and K.E. Cummings, "Adaption of FDTD techniques to acoustic modelling",11th Annu. Rev. Prog. Applied Computational Electromagnetics, Vol.2, 724 (1995)

[3] J.P. Berenger, "A perfectly matched layer for the absorption of electromagnetic waves'. J. Computational Physics, vol 114, 185-200, 1994.

[4] J.B. Schneider, C.L. Wagner, S.L. Broschat, "Implementation of transparent sources embedded in acoustic finite difference time domain grids", J. Acoust. Soc. Am Vol 133, No. 1, 136-142, January 1998.

[5] W.S.Lu, Y.Cui, R.L.Kirlin, "Least Pth Optimization for the design of 1-D filters with arbitrary amplitude and phase responses", ICASSP-93., 61 - 64 vol.3,1993

[6] A. Antoniou, Digital Filters: Analysis, Design, and Applications, Second Edition, McGraw-Hill, Inc. 1993.

[7] http://www.alglib.net/